# Risk-Aware Guidance of a Fixed-Wing UAV using Neural Network Model Predictive Control

Paul Bérard, Sylvain Bertrand, Baptiste Levasseur

# Risk-Aware Guidance of a Fixed-Wing UAV using Neural Network Model Predictive Control*

Paul Bérard[1], Sylvain Bertrand[1], Baptiste Levasseur[1]

***Abstract*— This paper presents a guidance algorithm for fixed-wing Unmanned Aerial Vehicles (UAVs) that accounts for risk wrt people at ground in case of failure of the vehicle. Model Predictive Control is used along with neural networks to predict online the ground risk probability associated to future trajectories. Guidance inputs are computed in this way for the UAV to follow a reference path while ensuring a given level of safety for the mission, despite flight conditions that may differ from mission preparation (wind, altitude, speed). Computation time concerns are accounted for in the design of the algorithm with the objective to facilitate a possible future implementation on board of an UAV. More precisely, neural networks are used for fast risk prediction, as well as systematic search for resolution of the MPC problem corresponding to the risk avoidance component of the control. Simulation results are proposed to illustrate the proposed approach.**

## I. INTRODUCTION

Fixed-wing Unmanned Aerial Vehicles (UAVs) can be used for long range operations such as linear infrastructure inspection, surveillance or delivery. These missions involve flights beyond visual line of sight for which a strong attention in their preparation must be payed, especially regarding risks that may be caused to third parties. Especially, there is a major concern regarding flights close to populated areas, that require a high level of safety to be ensured, both for the vehicle and the mission.

Methods have been proposed in the literature to be able to evaluate the risk induced by an UAV mission in a quantitative way. More specifically, probabilistic risk assessment is one of the most commonly adopted method by now for which dedicated models have been proposed [1][2][3]. A tool has been recently developed by the authors [4] that integrates such models for probabilistic risk evaluation wrt people [5] and road networks [6]. It has been used in the preparation of several UAV missions to assess the risks associated to given flight plans. In this mission preparation process, modifications of the flight plans are done by the operator to account for the results of the risk evaluation and define a new plan that satisfies the requirements.

Automatic computation or adaptation of a flight plan could be done by path planning approaches that have been developed in the literature and adapted to UAVs [7]. Classical path planning methods aim at finding a path or a trajectory in a constrained environment accounting for the presence of obstacles. Extensions of these methods have been more recently proposed to account for risk in the generation of a path or a reference trajectory.

The work of [8] proposes a path generation method based on the construction of visibility graphs on binary grid maps defined from geographical images to account for risk wrt to people and ground elevation. A Dijkstra algorithm is then used on the visibility graph to produce the path. In [9] a 3D path planning method is proposed by developing a risk-based A* algorithm. Different types of risks are considered, for people at ground, road vehicles, buildings, as well as a societal aspect (noise). Corresponding risk maps are generated and integrated in the evaluation of the cost function of the path planning algorithm. In [10], risk evaluation relies on the computation of a circular area that englobes possible impact points at ground. Influence of altitude and wind speed is taken into account to set the radius of this disk and the width of a corridor around a flight trajectory determined to avoid zones at risks (populated, no-fly zones, etc.). A RRT$^{\#}$ path planner with 3D Dubin curves is proposed in [11] to handle the trajectory generation problem while accounting for risks at ground. The risk evaluation accounts for ground impact probability distributions that may depend on the flight altitude and attitude angles of the vehicle. The algorithm is evaluated on the example of a take-off trajectory for a fixed-wing UAV. A RRT$^{*}$ algorithm is also proposed in [12] to generate risk-aware paths by considering different risk maps corresponding to populations, no-fly zones and obstacles.

In most of the existing approaches[1], maps of population density or risk maps are generated first and used as static inputs of the path finding or trajectory generation algorithm. A major issue is that the risk strongly depends on flight conditions. For instance, the size of the ground impact area and the probability distribution inside are strongly affected by the flight speed and altitude of the drone and by wind speed and direction (eg. see [13]). If during the flight these conditions remain the same as the ones assumed for path planning during mission preparation, then the expected level of safety will be guaranteed. But in practice, aerological conditions may strongly change during the flight and differ from the ones expected during mission preparation. Trajectory variations may also occur during the flight, eg. due to a reaction to unexpected events (return-to-home in straight line from current position, need to enter in a wait pattern,

*Part of this work was supported by French grant ANR Delicio (ANR-19-CE23-0006).

[1]All authors are with Université Paris-Saclay, ONERA, Traitement de l'Information et Systèmes, 91123, Palaiseau, France paul.berard@supelec.fr, { sylvain.bertrand, baptiste.levasseur}@onera.fr

[1]excepted from [10] and [11] where influence of a subset of the flight parameters is considered on the ground impact area or probability distribution.

change in the altitude to avoid communication issues with ground control station, etc.). In case of such changes during the mission, the level of safety defined and verified in mission preparation may also not be guaranteed anymore.
A first solution would consist in re-planning a new trajectory for the UAV accounting for changes in these flight conditions and updates in the risk maps. Nevertheless, this solution may be time consuming and not efficient to account for short term changes and must be combined to a more reactive layer, as it is usually the case for classical obstacle avoidance problems. Therefore, this paper aims at proposing a guidance algorithm for a fixed-wing UAV accounting for risk in a reactive manner during the flight. It can be used as an additional safety layer embedded on board of the UAV to ensure a given level of safety, in addition to a risk-aware path planning algorithm. Model Predictive Control (MPC) has been naturally chosen to design this guidance algorithm, due to its ability to account for predictions and constraints in the control computation. MPC has been already used in the literature to design guidance algorithms for fixed-wing UAVS, eg. [14][15][16][17].
The main contributions of this work are the following. A nonlinear Model Predictive Controller is proposed for risk-aware guidance of a fixed wing UAV. Probability of the risk for people at ground is accounted for in the formulation of the MPC problem. Computation of predictions of this risk probability is done online by using neural networks designed in previous works by the authors [13][18]. More precisely, these neural networks enable accurate and fast computation of the probability of ground impact by also taking into account the influence of altitude and speed of the UAV, as well as wind direction and speed. The structure of the proposed guidance algorithm accounts for computation time concerns to facilitate future implementation on a UAV.

The paper is structured as follows. The next section provides some background on probabilistic evaluation of ground risk. Section III presents the proposed MPC guidance algorithm. Use of neural networks to predict the risk is detailed in Section IV. Before concluding remarks, Section V provides some simulation results and analysis, as a proof of concept of the proposed approach.

## II. BACKGROUND ON GROUND RISK EVALUATION

The risk considered in this paper is the one of getting casualties for people at ground due to the fall of a fixed-wing UAV after some critical failure during its flight. More precisely, loss of on-board power is considered in this paper as the most probable and first hazardous event that will lead to a non controlled descent to the ground of the vehicle. In case of presence of people inside the possible ground impact area, a collision between the vehicle and someone may occur, and this collision may lead to some (lethal) injury.
To assess the probability of the risk, a classical decomposition into these four conditional events is adopted: loss of control due to power failure, impact at ground, collision with someone, (fatal) injury to someone. The corresponding evaluation formula of the risk probability, introduced in early works such as [1] and now commonly used in the literature is therefore the following:

$$\Pr\{casualty\} = \Pr\{loss\}.\Pr\{impact\}.\Pr\{collision\} .\Pr\{injury\} \quad (1)$$

To assess the risk associated to a mission, this probability must be evaluated at each time instant of the flight, and for all locations inside possible ground impact areas. More information on the way to evaluate all the terms of (1) can be found eg. in [1][5].
In this paper, we are interested in developing a guidance algorithm to ensure that the risk encountered during the flight remains acceptable, that is to compute online guidance orders to be applied to the vehicle to possibly make the probability of risk decrease and remain below some pre-defined threshold. With this objective in mind, the risk equation (1) can be simplified.
Its first term, the probability of loss, is usually computed from a safety analysis of the vehicle, and may be considered constant during the mission. It is therefore assumed in this paper that the guidance algorithm will have no effect on this term, and without loss of generality it will be assumed for the rest of the paper that $\Pr\{loss\} = 1$.
The last term, the probability of getting (fatal) injury for someone, is often computed from a lethality model depending on the kinetic energy at impact [19], and therefore on the terminal velocity of the vehicle. For the sake of simplicity, a worst case scenario will be assumed in this paper, that is $\Pr\{injury\} = 1$.
Therefore, with these two assumptions, the following simplified risk equation will be used in this paper instead of (1):

$$\begin{aligned}\Pr\{casualty\} &= \Pr\{impact\}.\Pr\{collision\} \\ &= \Pr\{impact\}.S_{col}.\rho_{pop}\end{aligned} \quad (2)$$

where $S_{col}$ is the collision surface between the UAV and one person (assumed to be constant) [5], and $\rho_{pop}$ the population density at the location at ground where the risk is evaluated.
Once again, this simplified formula is adopted in this paper for the sake of the design of a risk-aware guidance algorithm and therefore considers the terms with the highest sensitivity to online modification of the trajectory of the UAV.
It is also worth mentioning that the guidance algorithm under consideration aims at controlling the vehicle during its "nominal" flight, i.e. when there is no failure, although accounting for a prediction of what would happen in case of failure thanks to (2). Since loss of power is considered as failure, it is assumed that guidance and control of the UAV are not effective anymore during its descent to the ground.

The next section is devoted to the formulation of the control problem and of the proposed guidance algorithm accounting for risk prediction.

## III. MPC GUIDANCE

### A. UAV Dynamics

In this paper, the guidance problem of a fixed-wing UAV is considered. It is assumed that a low level controller is used for inner-loop attitude control. Attitude dynamics of the UAV are therefore not accounted for in this work and a simplified 4-degrees-of-freedom model will be considered to represent the dynamics of the drone.

Let define by $p = [p^x\, p^y\, p^z]^\top$ the position of the drone in a local NED reference frame, $V$ its airspeed, $\gamma$ its flight path angle, $\phi$ its bank angle and $\chi$ its heading angle.

As in [16], it is assumed that the horizontal part of the motion of the drone can be decomposed into segments with constant curvature and that the vehicles performs steady horizontal turns with zero sideslip and small values of $\gamma$. A nonlinear discrete-time model is used, assuming constant speed, flight path angle and bank angle over a sampling period $T_s$:

$$p^x_{k+1} = p^x_k + T_s \frac{V_k \cos\gamma_k}{\kappa_k} \left(\sin(\kappa_k + \chi_k) - \sin\chi_k\right) \quad (3)$$

$$p^y_{k+1} = p^y_k + T_s \frac{V_k \cos\gamma_k}{\kappa_k} \left(\cos(\kappa_k + \chi_k) - \cos\chi_k\right) \quad (4)$$

$$p^z_{k+1} = p^z_k - T_s V_k \sin\gamma_k \quad (5)$$

$$\chi_{k+1} = \chi_k + \kappa_k \quad (6)$$

where $k$ denotes the time-index and

$$\kappa_k = T_s \frac{g \tan\phi_k}{V_k} \quad (7)$$

For $\kappa_k$ close to zero (i.e. $\phi_k$ close to zero, eg. straight line motion), the following equations are used instead:

$$p^x_{k+1} = p^x_k + T_s V_k \cos\gamma_k \cos\chi_k \quad (8)$$

$$p^y_{k+1} = p^y_k + T_s V_k \cos\gamma_k \sin\chi_k \quad (9)$$

$$p^z_{k+1} = p^z_k - T_s V_k \sin\gamma_k \quad (10)$$

$$\chi_{k+1} = \chi_k + \kappa_k \quad (11)$$

The system dynamics will be summarized as $x_{k+1} = f(x_k, u_k)$ with the state vector $x_k = [p^x_k \quad p^y_k \quad p^z_k \quad \chi_k]^\top$ and the control input vector $u_k = [V_k \quad \gamma_k \quad \kappa_k]^\top$.

### B. Definition of the control problem

Following [16], the reference path to be tracked is assumed to be defined as a set of reference positions $p^r_i, i \in \mathbb{N}$ organized in a succession of different line segments. Let $r_k$ be the first point of the current reference path segment and $p^r_k$ the current point to be tracked on this segment at time index $k$ (see [16] for more details).

To represent the error between the position $p_k$ of the UAV and $p^r_k$ a lateral error vector is defined as

$$\epsilon^{lat}_k = n^r_k \times (p_k - r_k) \quad (12)$$

with the unit vector

$$n^r_k = (p_k - r_k) / \|p_k - r_k\| \quad (13)$$

and a longitudinal algebraic error is defined as

$$\epsilon^{long}_k = (n^r_k)^\top (p_k - p^r_k) \quad (14)$$

The objective of the path tracking controller is to drive these errors to zero.

For the sake of simplicity, perturbations due to wind are not explicitly considered in the guidance algorithm presented in this paper. It is assumed that the low level controller is able to estimate wind disturbances and compensate their effects on the UAV trajectory. Nevertheless, in this work, wind is taken into account at the guidance level in the prediction of the risk at ground since, after a failure leading to a descent of the drone to the ground, wind compensation by the autopilot may not be guaranteed anymore.

The next section presents the proposed Model Predictive Control algorithm for risk-aware guidance.

### C. Model Predictive Controller for Risk-Aware Guidance

At time index $k$, the control input applied for UAV guidance is decomposed into two components

$$u_k = u^*_k + \mathbf{1}^{risk}_k \Delta u^*_k \quad (15)$$

The first component $u^*_k$ will ensure path tracking without considering risk, while the control deviation $\Delta u^*_k$ is computed and applied only if the predicted probability of casualty (see Section IV-B for its computation) becomes greater than a given threshold:

$$\mathbf{1}^{risk}_k = \begin{cases} 1 & \text{if} \quad \overline{Pr}\{casualty\}_k \geq \delta_{risk} \\ 0 & \text{else} \end{cases} \quad (16)$$

The component $u^*_k$ is obtained as the first term of the optimal control sequence $\{u^*\}_k^{k+N-1} = \{u^*_k, u^*_{k+1}, \ldots, u^*_{k+N-1}\}$ solution to the following MPC problem $\mathcal{P}^{track}_k$ for path tracking:

$$\min_{\{u\}_k^{k+N-1}} \quad J^{track}_k \quad (17)$$

$$\text{s.t.} \quad \bar{x}_{k+i+1} = f(\bar{x}_{k+i}, u_{k+i}), i = 0, .., N-1 \quad (18)$$

$$\bar{x}_k = x_k, \bar{x}_{k+i+1} \in \mathbb{X} \quad (19)$$

$$u_{k+i} \in \mathbb{U}, (u_{k+i+1} - u_{k+i}) \in \Delta\mathbb{U} \quad (20)$$

The cost function $J^{track}_k$ is decomposed as

$$J^{track}_k = J^{lat}_k + J^{long}_k + J^u_k \quad (21)$$

$$J^{lat}_k = \sum_{i=1}^{N} \left(\epsilon^{lat}_{k+i}\right)^\top Q^{lat} \epsilon^{lat}_{k+i} \quad (22)$$

$$J^{long}_k = \sum_{i=1}^{N} q^{long} \left(\epsilon^{long}_{k+i}\right)^2 \quad (23)$$

$$J^u_k = \sum_{i=1}^{N-1} \left(u_{k+i} - u_{k+i-1}\right)^\top R \left(u_{k+i} - u_{k+i-1}\right) \quad (24)$$

where $Q^{lat}$ and $R$ are positive definite weighting matrices and with $q^{long} > 0$.

From the solution $\{u^*\}_k^{k+N-1} = \{u^*_k, u^*_{k+1}, \ldots, u^*_{k+N-1}\}$ of $\mathcal{P}^{track}_k$ the corresponding predicted trajectory $\{\bar{x}^*\}_k^{k+N} = \{\bar{x}^*_k, \bar{x}^*_{k+1}, \ldots, \bar{x}^*_{k+N}\}$ is computed using (18) starting from $\bar{x}^*_k = x_k$.

The probability $\overline{Pr}\{casualty\}_k$ is computed to evaluate the risk along this predicted trajectory, with the method explained in Section IV-B. As previously mentioned, if this probability exceeds some threshold (16), the second component $\Delta u_k^*$ of (15) is computed by considering a second MPC problem $\mathcal{P}_k^{risk}$:

$$\min_{\{\Delta u\}_k^{k+N-1} \in \mathcal{S}_{\Delta u}} \quad J_k^{track} + J_k^{risk} \tag{25}$$

$$\text{s.t.} \quad \bar{x}_{k+i+1} = f(\bar{x}_{k+i}, u_{k+i}), i = 0, .., N-1 \tag{26}$$

$$u_{k+i} = u_{k+i}^* + \Delta u_{k+i} \tag{27}$$

$$\bar{x}_k = x_k, \bar{x}_{k+i+1} \in \mathbb{X} \tag{28}$$

$$u_{k+i} \in \mathbb{U}, (u_{k+i+1} - u_{k+i}) \in \Delta\mathbb{U} \tag{29}$$

From the solution $\{\Delta u^*\}_k^{k+N-1}$, only the first value $\Delta u_k^*$ is retained for (15). The cost $J_k^{risk}$ is chosen as

$$J_k^{risk} = q^{risk} \overline{Pr}\{casualty\}_k \tag{30}$$

with $q^{risk} > 0$ and where the predicted probability of getting casualties is computed along the predicted trajectory of the UAV, as described in Section IV-B.

Note that the minimization of (25) is done by considering a systematic search over a finite set $\mathcal{S}_{\Delta u}$ of predefined control sequences $\{\Delta u\}_k^{k+N-1}$. This set is pre-computed in advance to enable deviations with respect to a nominal trajectory. This systematic search procedure enables to reduce and bound the computation time. Indeed, a classical optimization could be time prohibitive when considering here the computation of the predicted risk in the cost evaluation, even while using neural networks with fast computation time as proposed in this work.

*Remark:* The final objective of a risk-aware guidance algorithm is to ensure that the probability of getting casualties does not exceed some threshold (eg. equivalent level of safety compared to manned aviation). This specification should be formalized as a constraint on the predicted probability into the MPC problem formulation. In this paper, a penalty in the cost function (25) has been chosen instead to avoid hard constraints that could lead to infeasibility of the optimization problem. This is a practical approach, for this first proof of concept of a risk-aware guidance algorithm, and MPC formulation with constraint on the predicted probability will be considered in future work.

## IV. GROUND RISK PREDICTION USING NEURAL NETWORKS

### A. Neural networks for ground impact probability computation

For a given time instant, the computation of ground impact probabilities must be done at each possible impact location inside the ground impact area. This computation may be done by assuming simple distributions such as Gaussian ones, but to the cost of a strong lack of accuracy. Previous works done by the authors have investigated the use of a six degrees-of-freedom flight mechanics model to generate non controlled descent trajectories after failure and resulting ground impact probability maps by Monte Carlo (MC) simulations, accounting for the effect of wind. As presented in [13][18] these maps strongly depend on the flight altitude $h_0$ of the UAV at the instant of failure, on its speed $V_0$ and on the wind speed $V_w$ and direction (angle) $\theta_w$. Very different multimodal distributions result from different values of these parameters. An example of two maps taken from [18] are given in the left column of Fig. 1 for $h_0$ =150m, $V_0$ =20m.s$^{-1}$, without wind (top), and for a wind with $V_w$ =5m.s$^{-1}$ and $\theta_w = 3\pi/5$rad (bottom).

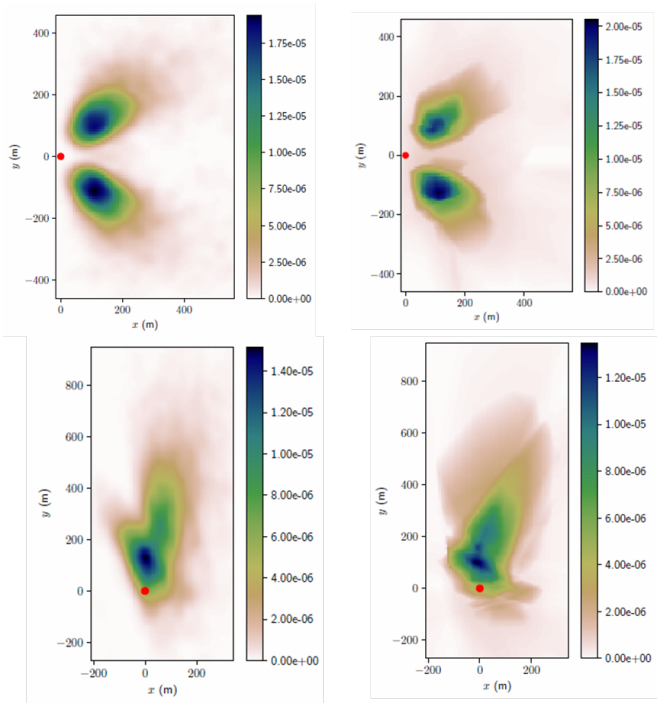


Fig. 1. Ground impact probability maps generated by Monte Carlo simulations (left column) and neural networks (right column) [18]

This generation process of ground impact probability maps by MC simulations is accurate but computationally time prohibitive[2] for an online use by a guidance algorithm. Neural networks have therefore been developed in [18] by the authors as surrogate models for fast computation. Two corresponding examples of maps obtained by these neural networks are given on the right column of Fig. 1.

A first neural network enables to compute the "boundaries" of the impact probability maps $(p_{min}^x, p_{max}^x, p_{min}^y, p_{max}^y) = f_1^{NN}(h_0, V_0, V_w, \theta_w)$ in a local reference frame associated to the UAV. A second neural network can be used to compute $Pr\{impact\} = f_2^{NN}((x,y),(h_0, V_0, V_w, \theta_w))$ at any location $(x, y)$ inside the boundaries.

These neural networks enable fast computation and they are used for evaluation of $\Pr\{impact\}$ and then prediction of

[2]or memory prohibitive if trying to embed on the UAV computer all the maps that could correspond to possible encountered flight conditions.

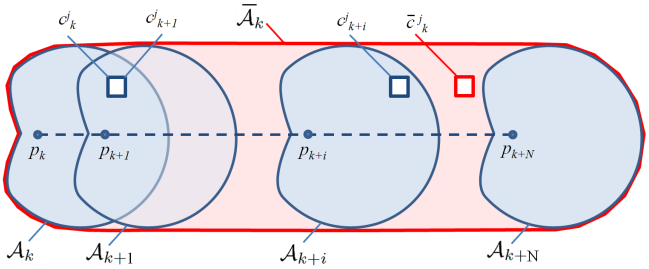


Fig. 2. Notations regarding predicted ground impact areas

$\overline{\Pr}\{casualty\}$ by the guidance algorithm, as described in the next section.

### B. Risk prediction

Let $\mathcal{A}_{k+i}$ be the ground impact area at time index $k+i$, $i = 0, \ldots, N$, corresponding to a failure of the UAV from the predicted position $p_{k+i}$. Assume that each area can be approximated by a partition of $n_i$ elementary cells $c^j_{k+i}, j = 1, \ldots, n_i$, corresponding to the resolution of the population density data (see Fig. 2):

$$\mathcal{A}_{k+i} = \bigcup_{j=1}^{n_i} c^j_{k+i} \tag{31}$$

For each prediction index $i$, $i = 0, \ldots, N$, the probability (2) is evaluated for each cell $c^j_{k+i}$ of $\mathcal{A}_{k+i}$: $\Pr\{casualty\}(c^j_{k+i})$. Let denote by $\bar{\mathcal{A}}_k$ the predicted ground impact area developed along the predicted trajectory, that is

$$\bar{\mathcal{A}}_k = \bigcup_{i=0}^{N} \mathcal{A}_{k+i} \tag{32}$$

Let us denote by $\bar{c}^j_k$ the set of $\bar{n}_k$ cells that define a partition of $\bar{\mathcal{A}}_k$:

$$\bar{\mathcal{A}}_k = \bigcup_{j=1}^{\bar{n}_k} \bar{c}^j_k \tag{33}$$

As one cell $\bar{c}^j_k$ may correspond to several cells $c^j_{k+i}$ of $\mathcal{A}_{k+i}$ for different indexes $i$ (impact areas along the predicted positions may overlap) the maximum value of the probability will be retained as a worst case

$$\begin{aligned} \Pr\{casualty\}(\bar{c}^j_k) = \max_i \{ & \Pr\{casualty\}(c^l_{k+i}) | \\ & i = 0, \ldots, N, \\ & l = 1, \ldots, n_i, \\ & c^l_{k+i} = \bar{c}^j_k \} \end{aligned} \tag{34}$$

Finally the predicted probability used in the cost function (30) is computed as the mean probability over the predicted ground impact area $\bar{\mathcal{A}}_k$:

$$\overline{\Pr}\{causalty\}_k = \frac{1}{\bar{n}_k} \sum_{j=1}^{\bar{n}_k} \Pr\{casualty\}(\bar{c}^j_k) \tag{35}$$

Note that a max value can also be used as a worst case, if preferable, instead of the mean value.

### C. Reducing computation time

Evaluation of the cost function $J^{risk}_k$ involves the computation of the probabilities of casualty over the ground impact area developed along the predicted trajectory. Although neural networks enable a fast computation of ground impact probabilities, a huge number of evaluations at different possible impact locations, for different flight conditions, is still required and may result in non negligible computation load.

Parallel computing of the predictions is one practical solution to this problem (see eg. [20]). In this paper, final implementation concerns are not addressed but some assumptions have been made with this goal in mind to reduce the computation load.

First, it is assumed that the wind can be considered constant (both in magnitude and direction) over the prediction horizon. Second, it is assumed that the same ground impact probability map can be used for altitude and speed variations of the UAV "small enough". A study on the influence of altitude and speed has been made to determine variation thresholds, respectively of 10m and $0.1\text{ms}^{-1}$, resulting in a maximum error of 10% on the probability map.

These assumptions enable to reduce the number of computations of different ground impact maps (and corresponding loads in memory of several different neural networks).

## V. SIMULATION EXAMPLES

Preliminary results are presented in this section as a proof of concept to illustrate the proposed approach. Lateral avoidance is considered here, i.e. the control deviation used in (15) is of the form $\Delta u^*_k = [0 \quad 0 \quad \Delta\kappa^*_k]^\top$. The set $\mathcal{S}_{\Delta u}$ is composed of 19 predefined candidate control sequences $\{\Delta\kappa\}_k^{k+N-1}$ leading to trajectory deviations presented in Fig. 3 in the case of an initial position at (0,0) and velocity directed along the $x$-axis. The parameters used for the MPC

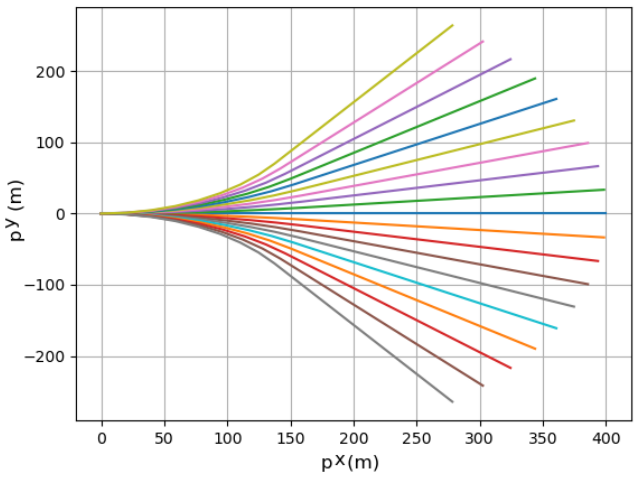


Fig. 3. Deviation trajectories resulting from application of candidate control sequences $\{\Delta u\}_k^{k+N-1} \in \mathcal{S}_{\Delta u}$.

guidance algorithm are presented in Table I. The constraint

sets $\mathbb{U}$ and $\Delta\mathbb{U}$ are defined from the min-max bound vectors, $\mathbf{u}_{min}$, $\mathbf{u}_{max}$, $\Delta\mathbf{u}_{min}$, $\Delta\mathbf{u}_{max}$ given in Table I. No state constraints have been considered for the simulations here.

| | |
|---|---|
| $N$ | 15 |
| $Q^{lat}$ | diag(10, 1, 0.1) |
| $q^{long}$ | 0.1 |
| $R$ | 20*diag(4.8, 7.28E2, 5.82E1) |
| $q^{risk}$ | 1E8 |
| $\mathbf{u}_{min}$ | $[15\ -0.15\ -0.2]^\top$ |
| $\mathbf{u}_{max}$ | $[25\ 0.15\ 0.2]^\top$ |
| $\Delta\mathbf{u}_{min}$ | $[-2.5\ -0.0524\ -0.131]^\top$ |
| $\Delta\mathbf{u}_{max}$ | $[2.5\ 0.0524\ 0.131]^\top$ |

TABLE I

PARAMETERS OF THE MPC GUIDANCE ALGORITHM

Regarding risk evaluation, the collision surface used in (2) is chosen as $S_{col} = 1\text{m}^2$, without loss of generality. Normalized values are considered for the population density $\rho_{pop}$, i.e. population density data is divided by its maximum value over the region of the considered scenario to get values of $\rho_{pop}$ in $[0, 1]$.

### A. Unit scenario

A first unit scenario is considered here in Fig. 4, where the UAV has to follow a linear reference path, at an altitude of 130m, with an initial nominal speed $V$ =20m.s$^{-1}$ and heading towards the $x$-axis. The reference path is represented by a grey dotted lined. Some populated areas are located in the vicinity of the reference path, and are represented by areas with color depending on the normalized population density.

In the case of no wind and no risk avoidance ($\delta_{risk} > 1$), the trajectory of the UAV (in red, with initial position depicted by a red dot) perfectly follows the reference path to be tracked thanks to tracking component $u_k^*$ computed by the MPC guidance. The ground impact probability maps $\mathcal{A}_k$ developed along the UAV trajectory is also plotted in Fig. 4, keeping the maximum value of the probability over time for each location at ground. In this case without wind one can notice two modes with greater probabilities located at each side of the UAV trajectory (as in Fig. 1, top part). As can be noticed, the ground impact probability maps intersects areas with "high" population densities. It results in some peaks for the predicted probability of casualty criterion (35), with a maximum value close to 1.6E-6 (see Fig. 5).

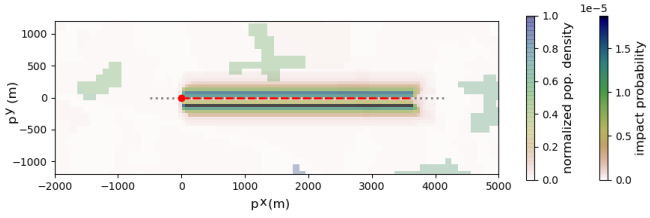


Fig. 4. Trajectory without wind - no risk avoidance

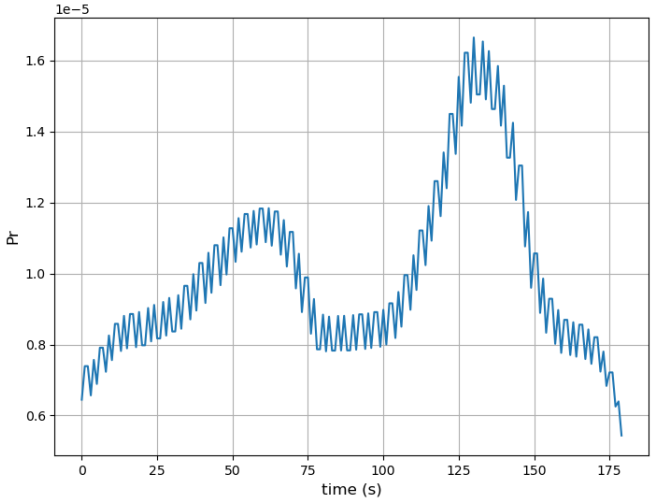


Fig. 5. $\overline{\Pr}\{casualty\}$ without wind - no risk avoidance

Let now consider the presence of a constant wind with velocity $V_w$ =5m.s$^{-1}$ and direction $\theta_w = \pi/2$ rad (wind directed upwards along the $y$-axis). As previously mentioned, wind compensation by the controller is out of the scope of this paper and it is assumed that the trajectory of the UAV is corrected. Nevertheless influence of wind is accounted for in the evaluation of the ground impact area. Indeed, as can be seen in Fig. 6, the distribution of the ground impact probabilities is not symmetric anymore with respect to the UAV trajectory, but areas with higher probabilities are now located in the "upper" side of the trajectory, due to wind. In this case, if no risk avoidance is still considered ($\delta_{risk} > 1$), ground impact areas with higher probabilities now intersect larger parts of populated areas. As a consequence, $\overline{\Pr}\{casualty\}$ increases, with a maximum greater than 7E-5 (see Fig. 7).

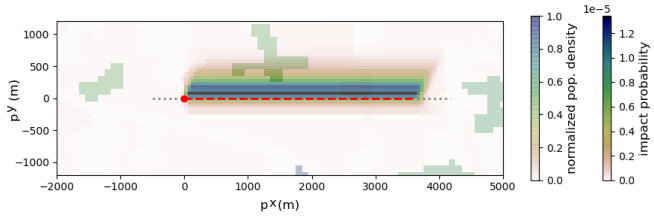


Fig. 6. Trajectory in presence of wind - no risk avoidance

Consider now the same scenario with risk avoidance by choosing $\delta_{risk}$ =5.10$^{-5}$. In that case, control deviations $\Delta u_k^*$ are computed and applied to the UAV to make the risk decrease. The risk avoidance trajectory performed by the UAV is presented on Fig. 8 resulting in a lateral deviation close to 160m from the reference path, but enabling to maintain the risk criterion below 5.10$^{-5}$ (see Fig. 9). As can be verified in Fig. 10 the control signals applied to the UAV satisfy the constraints (black dashed lines) thanks to the MPC formulation.

For this scenario with wind, maximum values of the lateral

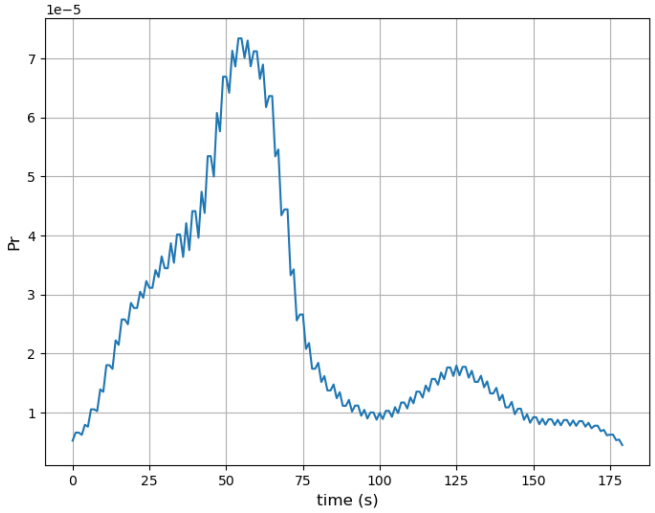


Fig. 7. $\overline{\Pr}\{casualty\}$ in presence of wind - no risk avoidance

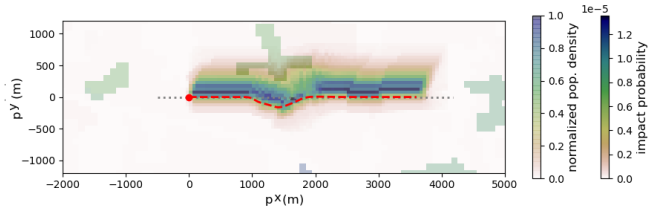


Fig. 8. Trajectory in presence of wind - avoidance with $\delta_{risk} = 5.10^{-5}$

deviation $\|\epsilon_{lat}\|$ with respect to the reference path are given in Table II, as obtained by simulations for different values of the probability threshold $\delta_{risk}$. As expected, the smaller the probability threshold is, the greater must be the deviation from the reference path.

### B. More complex scenario

Simulation results corresponding to one another scenario are presented here, in the case of a reference path composed of two linear segments. The second segment leads to a flight trajectory above a part of a populated area as can be seen in Fig. 11. The right lateral mode of the ground impact probability distribution intersects this part of the populated area. As can be seen in the blue curve of Fig. 12, it results in an increase of one order of magnitude in the risk probabilities, as evaluated using (2), from $\sim 10^{-5}$ over non populated areas to $\sim 1.4\ 10^{-4}$ over the populated area.
Assume a probability of failure $\Pr\{loss\} = 10^{-3}$ [5] and a worst case assumption $\Pr\{injury\} = 1$ regarding possible injuries to someone in the case of collision with

| $\delta_{risk}$ | 2e-5 | 3e-5 | 4e-5 | 5e-5 | 6e-5 |
|---|---|---|---|---|---|
| $\max_k \|\epsilon_k^{lat}\|$ (m) | 237.3 | 212.6 | 180.9 | 163.2 | 127.6 |

TABLE II

MAXIMUM LATERAL DEVIATION FROM REFERENCE PATH, DEPENDING ON RISK PROBABILITY THRESHOLD

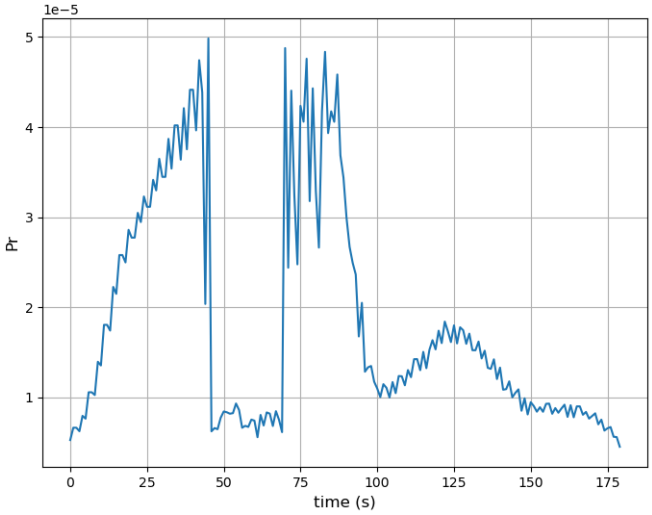


Fig. 9. $\overline{\Pr}\{casualty\}$ in presence of wind - avoidance with $\delta_{risk} = 5.10^{-5}$

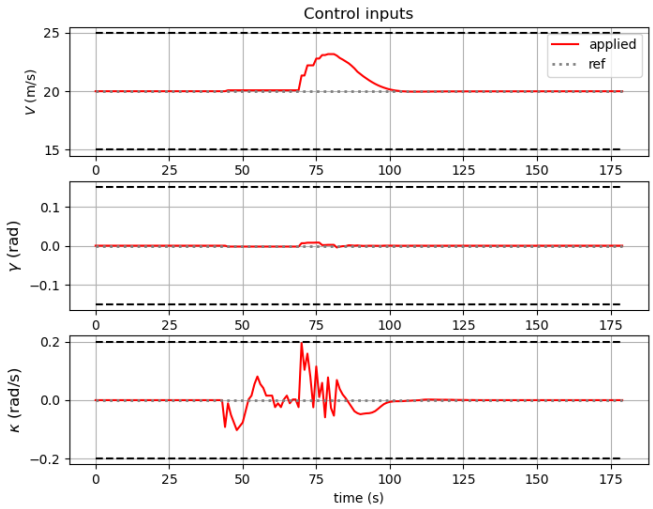


Fig. 10. Control inputs in presence of wind - risk avoidance with $\delta_{risk} = 5.10^{-5}$

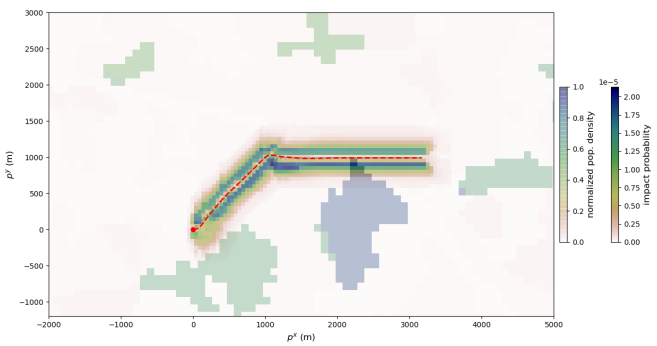


Fig. 11. Trajectory without risk avoidance

the UAV. If one is interested in ensuring an equivalent level of safety of the order of magnitude of $10^{-7}$, using the full

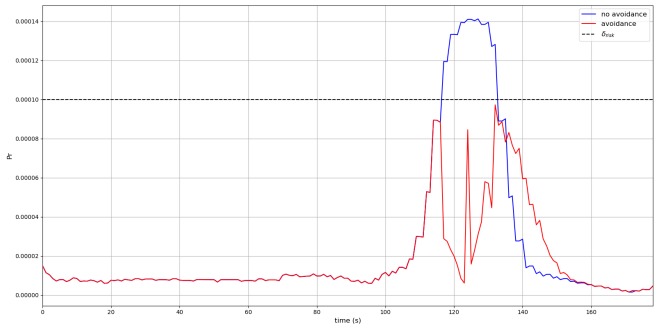


Fig. 12. Comparison of $\overline{\Pr}\{casualty\}$ without and with risk avoidance

risk equation (1) along with these assumptions leads to a threshold $\delta_{risk} = 10^{-4}$.

For this threshold, the proposed guidance algorithm makes the UAV locally deviate from the reference path (Fig. 13) enabling a risk probability below $10^{-4}$ (red curve on Fig. 12) compliant with the $10^{-7}$ objective when considering the two other terms of the full risk equation (1).

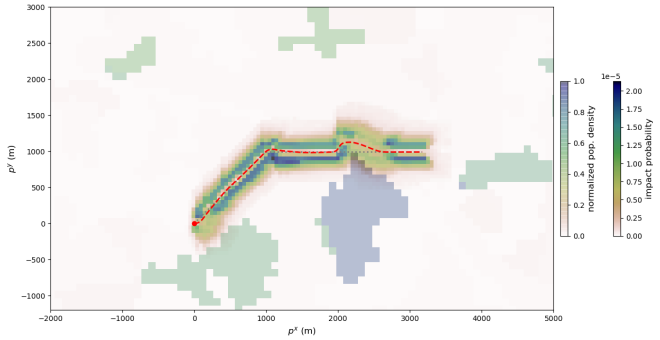


Fig. 13. Trajectory with risk avoidance

Deviations applied to control inputs for risk avoidance can be visible in Fig. 14 as well as satisfaction of the constraints depicted by the black dashed curves.

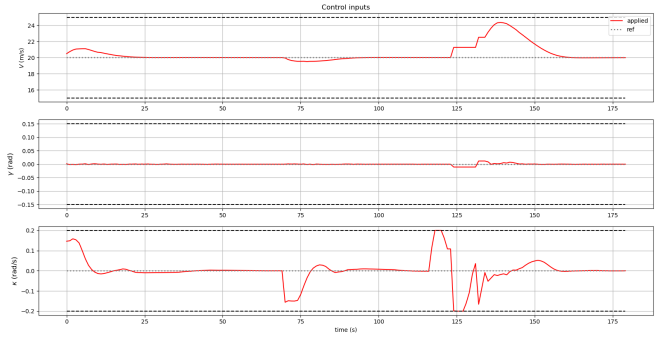


Fig. 14. Control inputs for the case with risk avoidance

## VI. CONCLUSION

This paper has presented a risk-aware guidance algorithm for a fixed-wing UAV based on model predictive control and neural networks. It enables to predict online the ground risk probability associated to future trajectories and account for it in the computation of the guidance control inputs. The main purpose of this algorithm is to ensure a given level of safety during a mission despite flight conditions (wind speed or direction, drone speed or altitude) that may change and differ from mission preparation. Computation time concerns have been considered for the development of the proposed approach to facilitate a future real time implementation on-board of a drone and serve as an additional layer of safety for UAV operations close to populated areas.

Future work will focus on 3D avoidance and state constraints, wind compensation in the MPC guidance algorithm. Evaluation on more complex scenarios, combined with a mission preparation based on risk-evaluation, are also under consideration.

## REFERENCES


[1] R. Clothier, R. Walker, N. Fulton and D. Campbell, "A Casualty Risk Anlysis for Unmanned Aerial System Operations over Inhabited Areas", Twelfth Australian International Aerospace Congress, 2nd Australasian Unmanned Air Vehicles Conference, 2007.

[2] P. Wu and R. Clothier, "The development of ground impact models for the analysis of the risks associated with Unmanned Aircraft Operations over inhabited areas", European Safety and Reliability Conference, Helsinki, Finland, 2012.

[3] R. Melnyk, D. Schrage, V. Volovoi and H. Jimenez, "A third-party casualty risk model for unmanned aircraft system operations", in Reliability Engineering & System Safety, vol.124, pp.105-116, 2014.

[4] N. Raballand, S. Bertrand, S. Lala and B. Levasseur, "DROSERA: a DROne Simulation Environment for Risk Assessment", European Safety and Reliability Conference, Angers, France, 2021.

[5] S. Bertrand, N. Raballand, F. Viguier and F. Muller, "Ground Risk Assessment for Long-Range Inspection Missions of Railways by UAVs", International Conference on Unmanned Aircraft Systems, Miami, USA, 2017.

[6] S. Bertrand, N. Raballand and F. Viguier, "Evaluating Ground Risks for Road Networks Induced by UAV Operations", International Conference on Unmanned Aircraft Systems, Dallas, USA, 2018.

[7] C. Goerzen, Z. Kong and B. Mettler, "A Survey of Motion Planning Algorithms from the Perspective of Autonomous UAV Guidance", in Journal of Intelligent & Robotic Systems, vol.57, pp.65-100, 2010.

[8] F.L.L. Medeiros, J.D.S.D. Silva, "Computational Modeling for Automatic Path Planning Based on Evaluations of the Effects of Impacts of UAVs on the Ground", in Journal of Intelligent & Robotic Systems, vol.61, pp.181–202, 2011.

[9] B. Pang, X. Hu, W. Dai and K.H. Low, "Third Party Risk Modelling and Assessment for Safe UAV Path Planning in Metropolitan Environments", preprint arXiv 2107.01834, 2021.

[10] C.E. Lin and P.C. Shao, "Failure Analysis for an Unmanned Aerial Vehicle Using Safe Path Planning", in Journal of Aerospace Information Systems, vol.17, no.7, pp.358-369, 2020.

[11] E. Rudnick-Cohen, S. Azarm and J. H. Herrmann, "Planning Unmanned Aerial System (UAS) Takeoff Trajectories to Minimize Third-party Risk", International Conference on Unmanned Aircraft Systems, Atlanta, GA, USA, 2019.

[12] S. Primatesta, L. S. Cuomo, G. Guglieri and A. Rizzo, "An Innovative Algorithm to Estimate Risk Optimum Path for Unmanned Aerial Vehicles in Urban Environments", in Transportation Research Procedia, vol.35, pp. 44-53, 2018.

[13] B. Levasseur, S. Bertrand, N. Raballand, F. Viguier and G. Goussu, "Accurate Ground Impact Footprints and Probabilistic Maps for Risk Analysis of UAV Missions", IEEE Aerospace Conference, Big Sky, Montana, USA, 2019.

[14] I. Prodan, S. Olaru, R. Bencatel, J. Borges de Sousa, C. Stoica, S.I. Niculescu, "Receding horizon flight control for trajectory tracking of autonomous aerial vehicles", in Control Engineering Practice, vol.21, no.10, pp.1334-1349, 2013.

[15] P. Oettershagen, A. Melzer, S. Leutenegger, K. Alexis and R. Siegwart, "Explicit model predictive control and L1-navigation strategies for fixed-wing UAV path tracking," 22nd Mediterranean Conference on Control and Automation, 2014.

[16] F. Gavilan, R. Vazquez and E. F. Camacho, "An Iterative Model Predictive Control Algorithm for UAV Guidance", in IEEE Transactions on Aerospace and Electronic Systems, vol.51, no.3, pp.2406-2419, 2015.

[17] T. Stastny, A. Dash, and R. Siegwart, "Nonlinear MPC for Fixed-wing UAV Trajectory Tracking: Implementation and Flight Experiments", AIAA Guidance Navigation and Control Conference, 2017.

[18] B. Levasseur, S. Bertrand, N. Raballand, "Efficient Generation of Ground Impact Probability Maps by Neural Networks for Risk Analysis of UAV Missions", International Conference on Unmanned Aircraft Systems, Athens, Greece, 2020.

[19] K. Dalamagkidis, K. P. Valavanis and L. A. Piegl, "Evaluationg the Risk of Unmanned Aircraft Ground Impacts", 16th Mediterranean Conference on Control and Automation, 2008.

[20] D.K. Phung, B. Hérissé, J. Marzat and S. Bertrand, "Model Predictive Control for Autonomous Navigation using Embedded Graphics Processing Unit", 20th IFAC World Congress, Toulouse, France, 2017.